Distributions of Radial Peripapillary Capillary Density and Correlations with Retinal Nerve Fiber Layer Thickness in Normal Subjects

Authors' Contribution:
Study Design A
Data Collection B
Statistical Analysis C
Data Interpretation D
Manuscript Preparation E
Literature Search F
Funds Collection G

ABCE **Guodong Liu***
BC **Yanliang Wang***
AE **Peng Gao**

Department of Ophthalmology, Shanghai Tenth People's Hospital Affiliated with Tongji University, Shanghai, PR China

Corresponding Author:
Financial support:
Conflict of interest:

* Guodong Liu and Yanliang Wang are co-first authors and contributed equally to this study
Peng Gao, e-mail: neocloudy@hotmail.com
This work was supported by the National Natural Science Foundation of China (No. 81700840)
None declared

Background:
The aim of this study was to investigate distribution rules of radial peripapillary capillaries (RPCs) density and correlations with retinal nerve fiber layers (RNFL) thickness in normal subjects.

Material/Methods:
We included 78 eyes of 78 healthy subjects examined by optical coherence tomography angiography (OCTA). RPCs density and RNFL thickness were measured automatically. Distributions of RPCs density and RNFL thickness were analyzed at different locations. Correlations of these 2 parameters and relationship with large vessels were evaluated by Spearman test.

Results:
Average density for overall, peripapillary, and inside disc RCPs was 56.12±2.51%, 58.56±2.84%, and 60.16±4.01%, respectively. Overall and peripapillary RCPs density were positively correlated with RNFL thickness (r=0.595, P<0.0001; r=0.578, P<0.0001). The highest RCPs density was found in the temporal quadrant and was lowest nasally, whereas the RNFL thickness was found to be lowest temporally and higher in the nasal region. However, a positive correlation was found in each sector, which was highest in the temporal inferior (r=0.550, P<0.0001). Large vessels were insignificantly correlated with both RCPs density and RNFL thickness in sector analysis.

Conclusions:
Although the distributions of RPCs density and RNFL thickness were different, a positive correlation was found in each sector. Distribution rules of RPCs density and RNFL thickness were related to both vascular-structure and activity-vascular.

Keywords:
Radial Peripapillary Capillary Density • Retinal Nerve Fiber Layer Thickness • Optical Coherence Tomography Angiography • Vascular Structural Relationship

Full-text PDF:
https://www.medscimonit.com/abstract/index/idArt/933601

📄 3131   ▦ 3   📊 6   📚 25

Background

Radial peripapillary capillaries (RPCs) are the vascular network located within the retinal nerve fiber layers (RNFL), which are visualized as the parallel vessels in the pattern of ganglion axons [1]. The correlations between RPCs density and RNFL thickness have been widely reported in vivo [2], in vitro [3], and in healthy [4] and in pathological retinas [5]. Previous studies demonstrated relatively similar conclusions, showing that RPCs density was positively associated with the RNFL thickness by histological and OCT images [3,6,7]. It is well known that RNFL thickness surrounding the optic disc follows "ISNT" rules [8,9]; however, whether RPCs have similar distribution rules remains uncertain. RNFL abnormal change is one of the most important clues to glaucoma diagnoses, whether RPCs density changes can be another sensitive parameter to predict glaucoma changes.

Currently, optical coherence tomography angiography (OCTA) provides a convenient method to visualize the retina vascular networks noninvasively. A number of studies have used OCTA to visualize retinal vasculature in peripapillary areas, showing the decrease of RPCs density corresponds with the thinning of RNFL thickness in glaucoma eyes [10-12]. However, whether RPCs density has similar distribution rules, and the correlations of RPCs density and RNFL thickness in vivo normal retinas are less studied [2,4,13].

Thus, the present study aimed to investigate the distribution characteristics of RPCs network at different locations in normal retinas and the possible correlations with RNFL thickness and large vessels in each sector by use of OCTA.

Material and Methods

Study Design and Subjects

We analyzed 78 eyes (the right eye only) from 78 individuals without retinal and systemic diseases. The detailed ophthalmic information, including best corrected visual acuity (BCVA), intraocular pressure (IOP), slit lamp biomicroscopy, fundus photography and OCTA scans, were recorded. BCVA of the subjects was better than 20/20, with the spherical equivalent less than 3 diopters in both eyes, while IOP was under 21 mmHg measured using a non-contact tonometer (Canon TX-2P, Tokyo, Japan) to exclude glaucoma or ocular hypertension.

We used the OCTA (Optovue, Inc., Fremont, CA), which has a light source spectrum of 840 nm and a bandwidth of 45 nm with an axial resolution of 5 um. The module of Angio disc scans with 4.5×4.5 mm area, centered on the optic nerve, was selected to examine optic vascular density. The algorithm of split-spectrum amplitude-decorrelation angiography (SSADA)

incorporated into the OCT advice was used to automatically segment the ONH vessels into 4 layers: vitreous, superficial, RPCs, and choroid. Vascular density was defined as a percent of the proportion of the examined area occupied by retinal vessels. Motion correction technology was used to remove the motion artifacts by horizontal and vertical scans. Images with quality signal strength index (SSI) lower than 8/10 were excluded due to media opacities or poor cooperation. Subjects taking any systemic medicines that affect the blood flow were also excluded in the present study. Also, relevant morphometric criteria such as "cup to disc ratio <0.5" were adopted to exclude possible clinical or subclinical glaucoma. The study was conducted in accordance with the tenets of the Declaration of Helsinki and was approved by the board of Shanghai Tenth People's Hospital (SHSY-IEC-KY-4.0/17-71/01). All the subjects involved in the study have given their written informed consent.
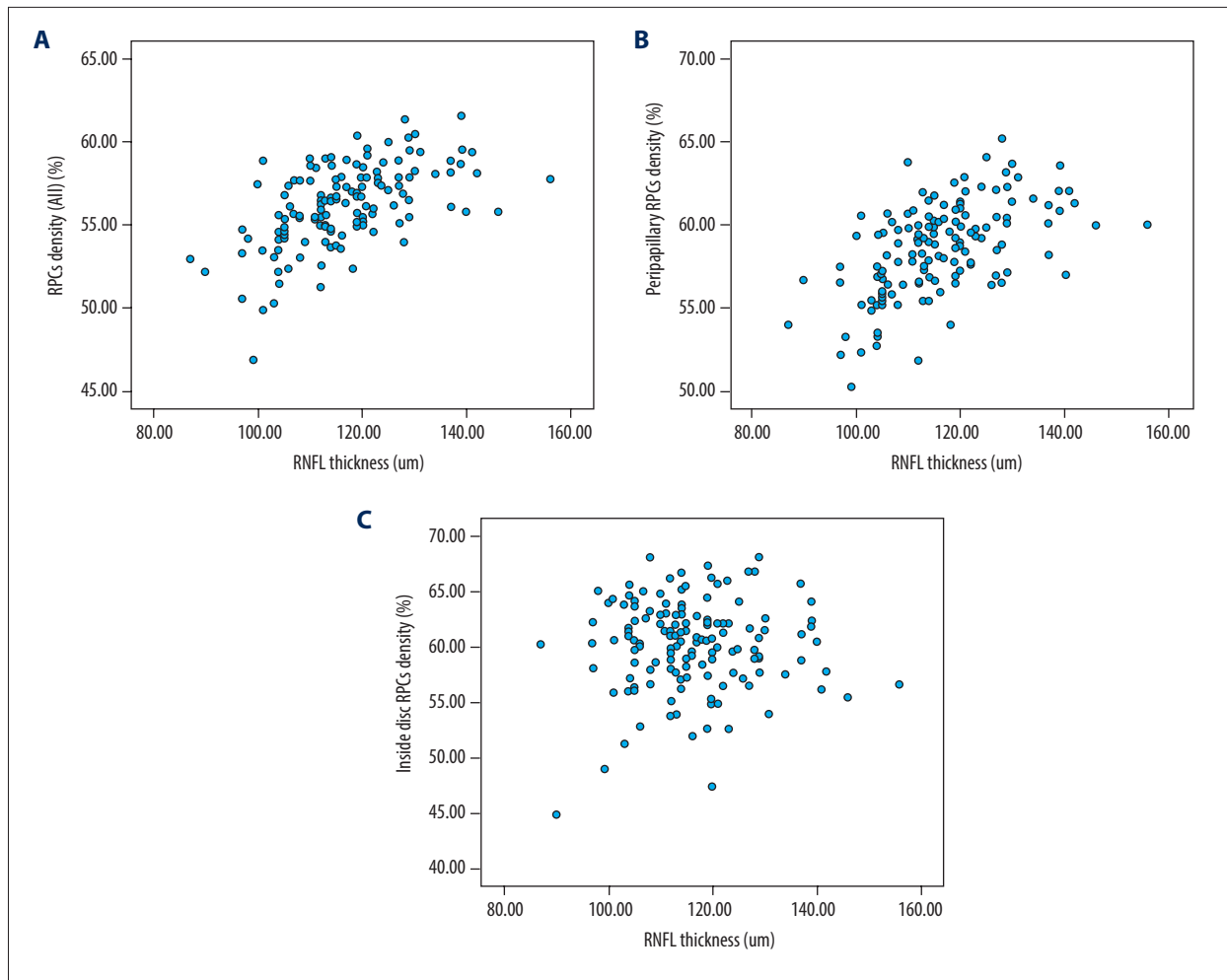
Measurements of RPCs Density and RNFL Thickness

Angio disc scan with a size of 4.5×4.5 mm was used to examine the ONH area. The flow density map software AngioAnalytics (version 2017.1.0.155) was used to quantify RPCs density within the distance from inner limiting membrane offset 0 μm to RNFL offset 0 μm automatically. The measurements of RPCs density and RNFL thickness were obtained in 4 equal quadrants: superior, temporal, inferior, and nasal; and 8 peripapillary sectors: nasal superior (NS), nasal inferior (NI), inferior nasal (IN), inferior temporal (IT), temporal inferior (TI), temporal superior (TS), superior temporal (ST), and superior nasal (SN) by modified Garway-Heath sector grid with 2 rings of 2 mm and 4 mm. Within the 2 mm area was defined as inside disc area, and the ring between 2 mm and 4 mm was the peripapillary region. RPCs density and RNFL thickness were recorded, and the corresponding distributions and correlations in each area were analyzed.

On the RNFL thickness map, arcuate regions look like butterfly wings because of warm color code with higher RNFL thickness. It is well accepted that the RNFL and RPCs are high within the arcuate regions because of the large vessels [3,7]. So, we furtherly investigated the possible contribution of big vessels on RNFL thickness and RPCs density. To better analyze the impacts of big vessel on RPCs density and RNFL thickness, we scored the large vessels with the following rules. The number of major vessels within ST and IT areas were scored as 2, major vessels with smaller lumen in SN and IN areas were scored as 1, and the first-grade branches and smaller vessel directly originating from optic dis were scored as 0.5. The relationship of vessel scores with RNFL thickness and RCPs were evaluated utilizing the Spearman test.

Statistical Analysis

Statistical analysis was performed using Statistical Package for the Social Sciences (SPSS) for Windows (version 27.0; IBM Inc.).

Figure 1. (**A-C**) Correlations between RCPs density and RNFL thickness. The blue scatterplots presented the correlations of RCPs density with RNFL thickness. Statistical Package for the Social Sciences (SPSS) for Windows (version 27.0; IBM Inc.).

Differences in RPCs density and RNFL thickness were tested by Mann-Whitney U test and one-way ANOVA. Correlations of RNFL thickness with RPC density, and influences of large vessels in each sector were analyzed using Spearman rank correlation. Values are presented as the mean±standard deviation (SD), and significance was assessed at the $P<0.05$ level.

Results

Basic Information and the Measurements

A total of 78 eyes of 78 normal Chinese subjects (40 males, 38 females) were included in this study. The mean age of all study participants was 43.7±9.9 years (range, 23-57 years).

Average overall RPCs density within the 4.5×4.5 mm was 56.12±2.51%, and the average peripapillary (within 2 mm ring) and inside disc (between 2 mm and 4 mm rings) RPCs density

was 58.56±2.84% and 60.16±4.01%, respectively. The mean RNFL thickness was 116.18±11.46 um. A positive correlation of RCPs density with RNFL thickness was obtained, ($r=0.595$, $P<0.0001$ for overall RPCs density; $r=0.578$, $P<0.0001$ for peripapillary RPCs density) (**Figure 1**). Although the values of inside disc RCPs density were similar with the peripapillary RPCs density ($P=0.356$), the correlations between inside disc RCPs density and peripapillary RPCs density ($r=0.08$, $P=0.352$) and RNFL thickness ($r=0.039$, $P=0.647$) were insignificant.
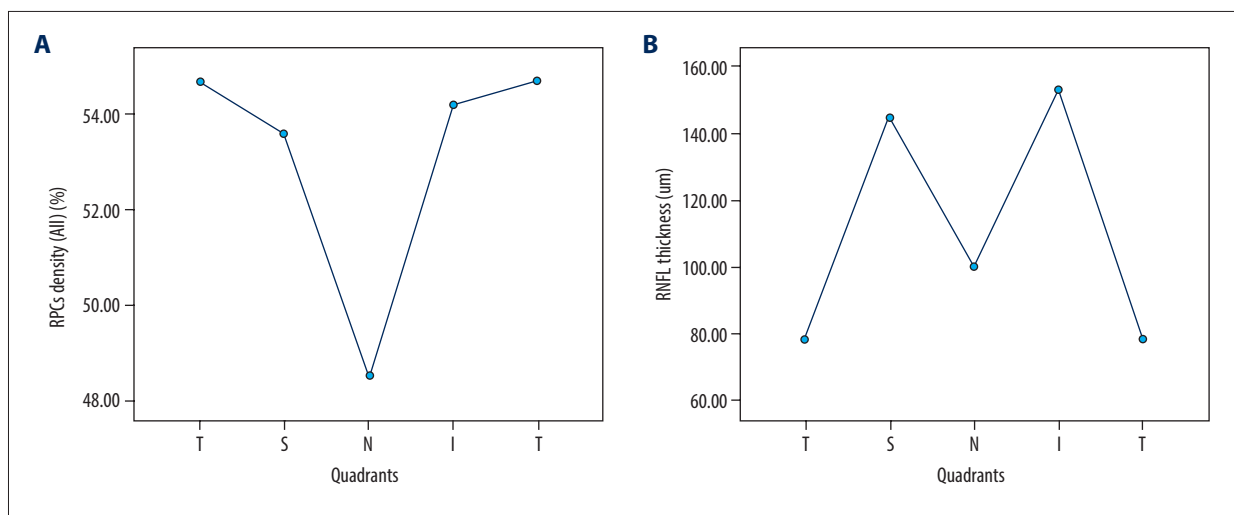
Distributions and Correlations of RPCs Density with RNFL Thickness in 4 Equal Quadrants

As expected, the average RNFL thickness followed "ISNT" rules, which was 150.15±18.92 um in inferior, 142.53±18.66 um in superior, 98.27±15.23 um in nasal, and 81.34±12.89 um in temporal, as shown in **Table 1**.

Table 1. Mean RPCs density and RNFL thickness in 4 equal quadrants (mean±SD).

Quadrants	T	S	N	I
RPCs density (%)	54.68±3.70	53.31±3.96	47.81±3.91	53.87±4.13
RNFL (um)	81.34±12.89	142.53±18.66	98.27±15.23	150.15±18.92
Spearman test	r=0.400, p<0.001	r=0.413, p<0.001	r=0.503, p<0.001	r=0.445, p<0.001

S – temporal; S – superior; N – nasal; I – inferior.

Figure 2. (**A, B**) Distributions of RCPs density and RNFL thickness in 4 equal quadrants. RPCs density was comparable in superior and inferior quadrants; the temporal density was much higher than nasal area. The thinnest RNFL thickness was found in temporal region, and the highest RNFL thickness in superior and inferior areas. Statistical Package for the Social Sciences (SPSS) for Windows (version 27.0; IBM Inc.).

The average RPCs density was found to be the thickness at the temporal region with the mean value of 54.68±3.70%, followed by inferior (53.87±4.13%) and superior (53.31±3.96%) quadrants, and the nasal area was the lowest (47.81±3.91%) (**Table 1**). Based on the measurements, the distribution of RPCs density was comparable between superior and inferior quadrants, but the temporal RPCs density was much higher than nasal region (*P*<0.0001, **Figure 2A**).

Something we did not anticipate was that the highest RPCs density was found in the temporal region where the thinnest RNFL were located (**Figure 2B**). So, the supposed positive correlation between RPCs and RNFL thickness was challenged, at least in the temporal area. However, in terms of each region, a moderate positive correlation was obtained, including temporal (r=0.400, *P*<0.001), superior (r=0.413, *P*<0.001), inferior (r=0.445, *P*<0.001), and nasal areas (r=0.503, *P*<0.001) (**Table 1**). The relationship between RCPs density and RNFL thickness was not as close as we had expected it to be, but still supports the typical structure-vascular relationship.

Distributions of RPCs Density and RNFL Thickness in 8 Sectors

Furthermore, we obtained the measurements of RPCs density and RNFL thickness in smaller regions utilizing the modified Garway-Heath sector grid (**Figure 3**). For RNFL thickness, the arcuate regions containing large vessels were thickest within ST, IT, SN, and IN, respectively. The thinnest RNFL thickness was found in temporal region with TS and TI (**Table 2**).

The RPCs density in ST and IT sectors was highest, but the areas containing more large vessels in SN and IN sectors were not as high as that in ST and IT sectors, and were even smaller than the temporal area (TS and TI sectors) without large vessels. The lowest values were found in nasal area (NS and NI sectors) (**Table 2**).

This reminded us to re-consider the contributions of large vessels to values of RPCs density. We recorded the number of large vessels in each sector except for the TS and TI areas because of the scarcity of large vessels in these 2 sectors.
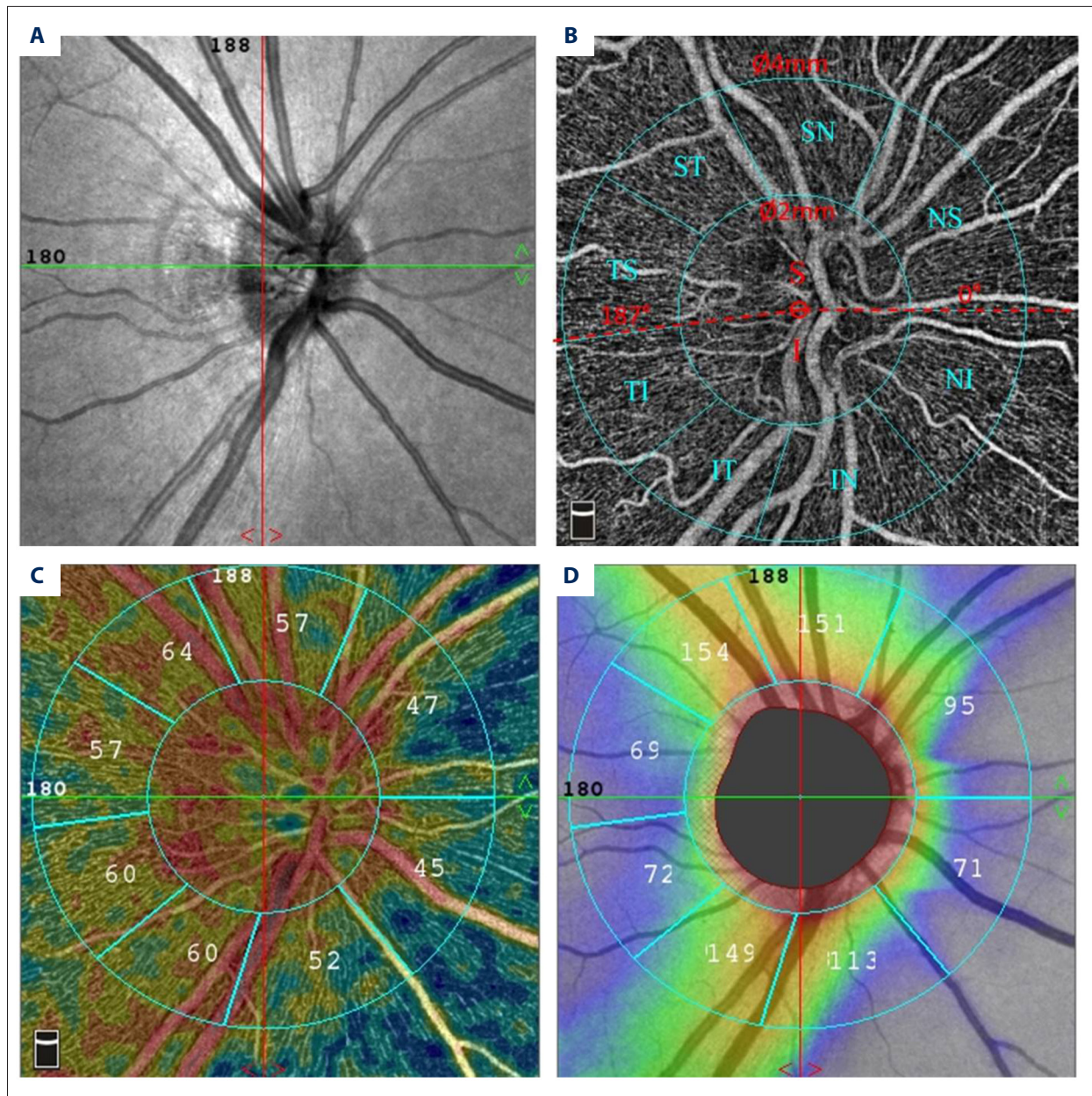
Figure 3. (**A-D**) RCPs density and RNFL thickness in modified Garway-Heath sectors. The Angio Disc RPCs enface image was separated by modified Garway-Heath sector grid into 8 sectors by 2 circles with a diameter of 2 mm and 4 mm. The picture was obtained from RTVue XR Avanti User Manual. Statistical Package for the Social Sciences (SPSS) for Windows (version 27.0; IBM Inc.).

Distribution of Large Vessels and Correlations with RPCs Density and RNFL Thickness

According to the grading roles (described in the Methods section), the highest score of large vessels was found in the SN sector, followed by IT and IN sectors (**Table 3**). These sectors were all located within arcuate areas, as expected. However, the score in ST sector was unexpected lower (2.25), where the greatest RPCs density was found. The result was consistent with the result that the correlation of RPCs density with RNFL thickness was low in the ST sector (r=0.153, P=0.071), indicating higher RPCs density with relatively smaller RNFL thickness. In terms of the contribution of large vessels on RPCs density and RNFL thickness, the Spearman results revealed insignificant correlations of large vessels with RPCs (r=-0.800, P=0.200) and RNFL thickness (r=0.194, P=0.806).

We randomly chose 2 individuals to analyze the distribution characteristics of large vessels, RNFL thickness, and RPCs density. In

Table 2. Mean peripapillary RPCs density and RNFL thickness in 8 modified Garway-Heath sectors (mean±SD).

Sectors	RPCs density (%)	RNFL (um)	Spearman test
ST	57.64±15.10	135.65±25.89	r=0.153, p=0.071
TS	56.13±3.93	82.51±13.38	r=0.454, p<0.0001
TI	53.14±4.45	79.71±15.82	r=0.550, p<0.0001
IT	57.01±4.42	156.96±24.18	r=0.200, p=0.018
IN	51.27±4.81	144.80±23.73	r=0.483, p<0.0001
NI	46.81±4.60	87.00±15.38	r=0.498, p<0.0001
NS	48.46±4.12	107.61±17.37	r=0.445, p<0.0001
SN	51.34±4.43	145.95±25.62	r=0.538, p<0.0001

ST – superior temporal; TS – temporal superior; TI – temporal inferior; IT – inferior temporal; IN – inferior nasal; NI – nasal inferior; NS – nasal superior; SN – superior nasal.

Table 3. Mean peripapillary RPCs density, RNFL thickness and vascular number in 6 sectors.

Sectors	RPCs density (%)	RNFL (um)	Vessel numbe
ST	57.64±15.10	135.65±25.89	2.25
IT	57.01±4.42	156.96±24.18	2.50
IN	51.27±4.81	144.80±23.73	2.93
NI	46.81±4.60	87.00±15.38	1.25
NS	48.46±4.12	107.61±17.37	2.41
SN	51.34±4.43	145.95±25.62	3.21

ST – superior temporal; IT – inferior temporal; IN – inferior nasal; NI – nasal inferior; NS – nasal superior; SN – superior nasal.

the first subject, the peak of RNFL thickness was in the ST sector and was close to that of the SN sector (**Figure 4A**), where the highest RNFL thickness and large vessels also appeared (**Figure 4B**). **Figure 4C** shows that the RPCs density in the ST sector without large vessels was higher than that in the SN sector. According to the rules, the score was 2 in the IT sector and 3 in the IN sector; however, the RNFL thickness and RPCs density in the IT sector were all higher than that in the IN sector (**Figure 4**).

In case 2, the peak of RNFL thickness was located in the middle of the ST sector (**Figure 5A**), where the thickest RNFL and highest RPCs density were found. However, the vessels score in the ST sector was lower than that in the SN sector. In the IT sector, the area without large vessels also showed thick RNFL according to the color map (**Figure 5B, 5C**). Therefore, although the large vessels were located in the arcuate area where RNFL converges, the contributions of large vessels to measurements of RPCs density and RNFL thickness was not as high as expected.

### Correlations and Trends of RPCs Density with RNFL Thickness in 8 Sectors

In agreement with the results in 4 quadrants, a moderate positive correlation was obtained in 8 sectors (**Table 2**). Our

analysis revealed the significant positive correlation between RCPs density and RNFL thickness, with the highest index in TI (r=0.550, *P*<0.0001). Compared with 4 quadrants, the correlation in 8 sectors was stronger (**Table 2**). Although the distributions of RPCs density and RNFL thickness were different, the trends of increases and decreases were similar (**Figure 6**).

Discussion

In the current study, we quantitatively demonstrated the measurements of RPCs density and RNFL thickness in 4 equal quadrants and 8 modified Garway-Heath sectors in normal human retinas. We investigated the distribution rules and possible correlations in each region. Previously, there were related articles reporting the distributions and correlation of RPCs density and RNFL thickness, but the values were inconsistent because of different quantitative methods and variable retinal conditions [2,3,14,15], such as smaller capillary diameters caused by fixated constriction or higher RPCs density due to low resolution [3]. Inspite of the discrepant results, the positively supportive correlations between RPCs density and RNFL thickness were widely accepted. In agreement with previous reports, we observed similar relationships between RCPs density and RNFL
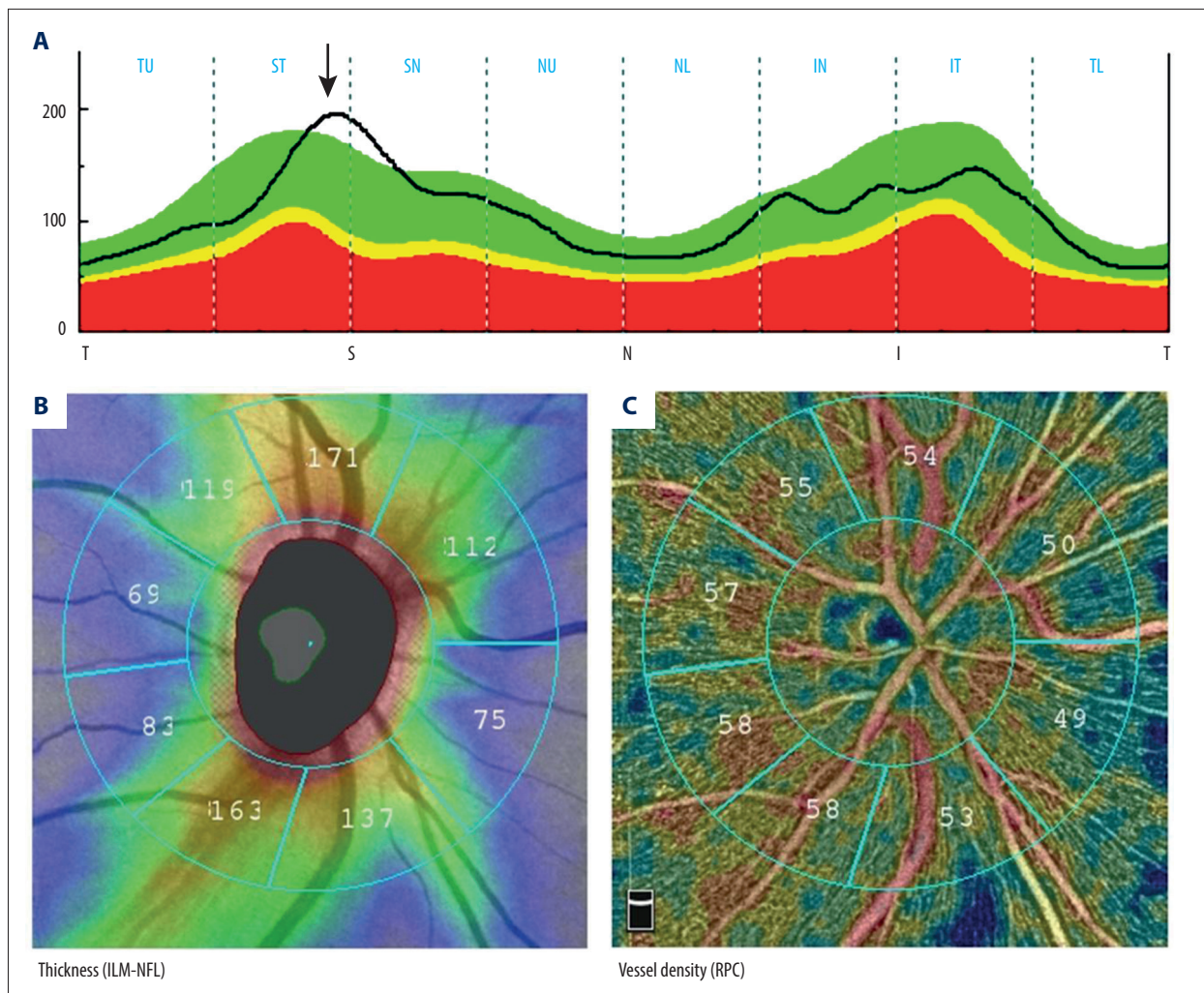
Figure 4. (**A-C**) A right eye of a young female (32 years old). The black arrow pointed out the location of highest RNFL thickness. Both capillaries and large vessels were included to calculate the regional density. Statistical Package for the Social Sciences (SPSS) for Windows (version 27.0; IBM Inc.).
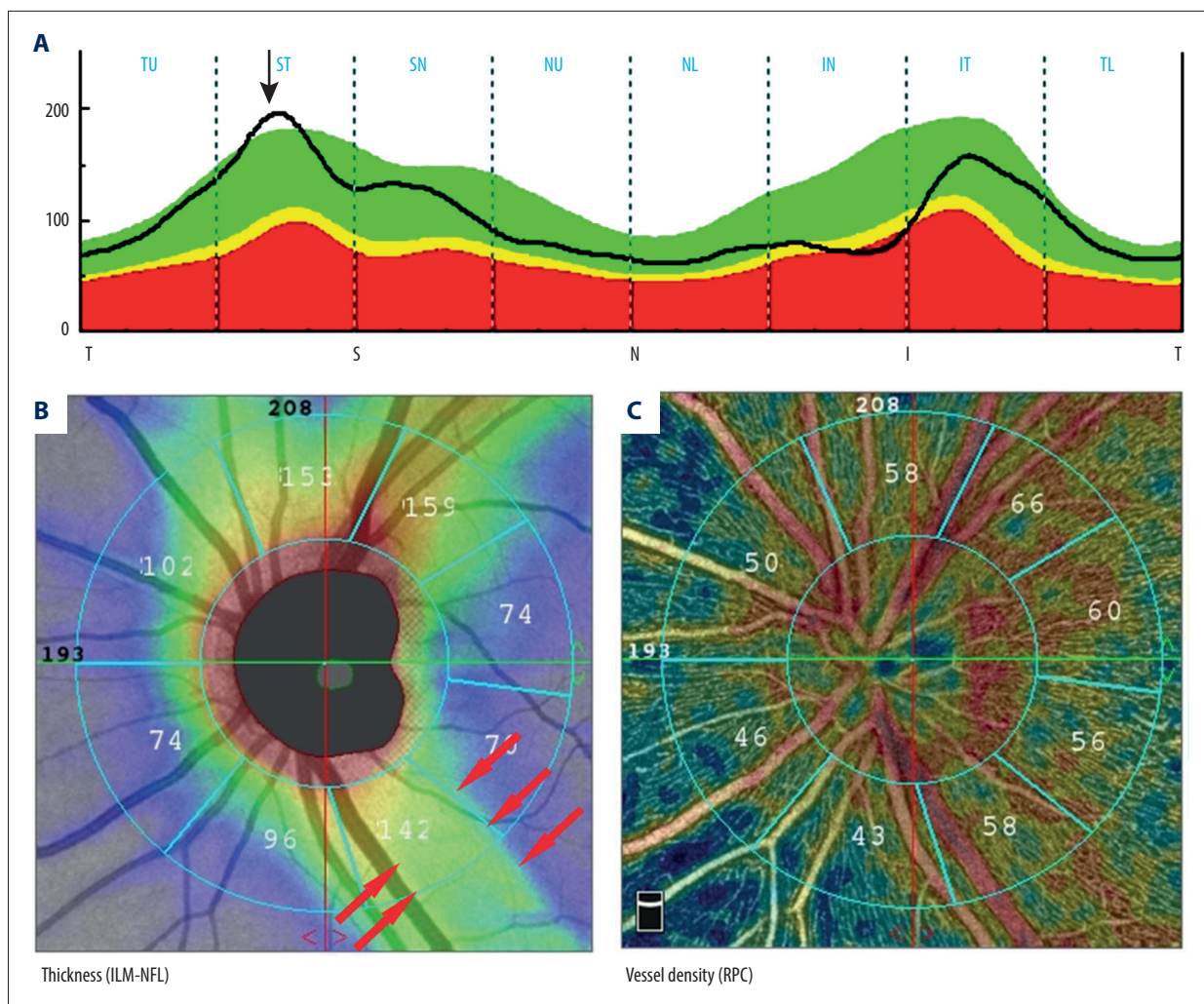
thickness (r=0.595, P<0.0001 for overall RPCs density; r=0.578, P<0.0001 for peripapillary RPCs density, respectively).

The inside RPCs converge into the optic nerve along with RNFL axons, so a close relationship of inside disc RCPs density with peripapillary RPCs density and RNFL thickness was proposed. However, the present results showed insignificant correlations of inside disc RCPs density with peripapillary RPCs density (r=0.08, P=0.352) or RNFL thickness (r=0.039, P=0.647). Inversely, the positive correlation between inside disc RCPs density and rim area has been reported in previous studies [16]. One of the reasons was that the rim area corresponded to the region where inside disc RPCs were distribution; therefore, a positive relationship between inside disc RPCs density and rim area was found because of the structure-vascular mechanism. The RNFL thickness in the present study was calculated within a 3.4-mm diameter circle centered on the optic nerve head. Therefore, the

extra area between 2 mm and 3.4 mm may influence assessment of the relationship between RPCs density and RNFL thickness.

To explain the low correlation between peripapillary and inside disc RPCs, the originations of capillaries within the ONH area were considered. The vascular network around the optic disk originates from both retinal and ciliary vessels, but both the peripapillary and inside disc RPCs mainly derive from the branches of the central retinal artery [17,18]; however vascular configurations were significantly different because of the various distances from the ONH [2].

The distributions of RNFL thickness followed the "ISNT" rules, as reported in the previous studies [9,19], that the RNFL thickness was high in the inferior region, followed by superior and nasal areas with temporal RNFL thickness is the thinnest. As a positive relationship between RCPs density and RNFL thickness

Figure 5. (**A-C**) A left eye of a middle-aged male (48 years old). The black arrow pointed out the location of highest RNFL thickness. Red arrows showed the area without big vessels, but showed warmer color. Statistical Package for the Social Sciences (SPSS) for Windows (version 27.0; IBM Inc.).
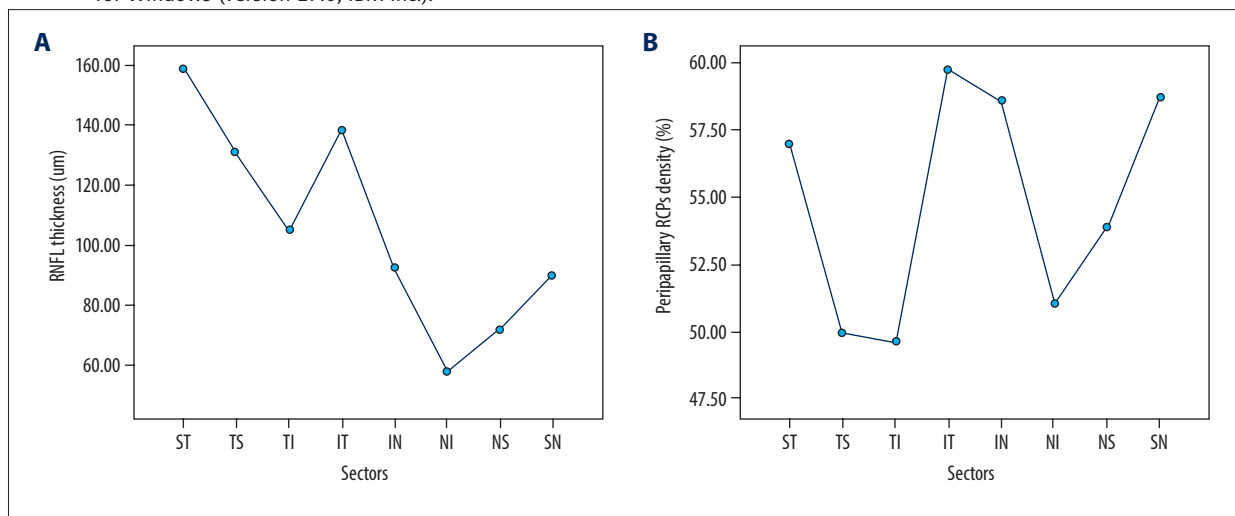
Figure 6. (**A, B**) Distributions of peripapillary RCPs density and RNFL thickness in 8 modified Garway-Heath sectors. The distribution of RNFL thickness was similar with the trend of peripapillary RPCs density with 2 lows and 3 highs at same points. (SPSS Statistics, version 22.0, IBM).

was proposed [6,7], a similar pattern of RPCs density with RNFL thickness distributions was anticipated.

Temporal RPCs density, however, turned out to be the highest when compared to other regions, where RNFL thickness was the thinnest. Inversely, while nasal RPCs density was lowest, nasal RNFL thickness was much thicker than in the temporal region. One plausible explanation for this opposite distribution is the activity-vascular related mechanism by which higher temporal RPCs exist to fulfill the highly metabolic requirements within the macular area. Inferior and superior RPCs densities were high and comparable, consistent with the distributions of RNFL thickness within the arcuate region. Nonetheless, we still detected positive correlations between RPCs density and RNFL thickness in each region, including temporal and nasal areas, supporting the vascular-structure relationship as proposed in previous studies [2-5].

In addition to the distributions and correlations in 4 quadrants, we investigated the parameters within smaller areas. The peripheral area was automatically separated into 8 sectors by the modified Garway-Heath sector grid. Corresponding RPCs density and RNFL thickness were then evaluated. Similarly, the most prominent RPCs density was found in the ST sector and IT sector, followed by the temporal area, and the lowest was found in the nasal area. In smaller regions, the difference of RNFL thickness between nasal and temporal areas was more significant, especially in the NS sector, when compared with TS sector. However, although the distribution rules of RPCs density and RNFL thickness were different, the trend to decrease or increase was similar in 8 sectors, showing a double-bottom at TI and NI sectors and 3 highs in ST, IT, and SN sectors. As a result, we proposed that the large vessels caused the regional highs of RPCs density and RNFL thickness, in agreement with previous studies [3,7].

However, our results revealed an insignificant correlation between high vascular scores with RPCs density and RNFL thickness. Given that highest RPCs density and RNFL thickness were found within or close to the arcuate regions, the contribution of big vessels to RPCs density and RNFL thickness was not as high as one would expect. When we reviewed the location of large vessels and distributions of RPCs density and RNFL thickness in individuals, we found that both the locations of highest RPCs density and RNFL thickness were inconsistent with large vessels. However, RNFL thickness was more prone to be related with large vessels, as large vessels were included in the measurement of RNFL thickness.

In accordance with the 4 quadrants, a positive correlation between RPCs density and RNFL thickness was identified in 8 sectors. The highest correlations were found in TI sector (r=0.550, $P<0.0001$), and the lowest in ST area (r=0.153, P=0.071). Therefore, even the distributions of RPCs density and RNFL thickness were almost opposite within the temporal area, and the highest structure-vascular correlation still exists in the region. ST area within the arcuate regions had the highest RPCs density and relatively high RNFL thickness, but the reasons behind the lowest correlation are unclear.

In immature retinas, astrocytes are the cells that establish the mesh-like network to support retinal vessel formation [20,21], which was guided by retinal ganglion cells [22,23]. We previously surmised that the thick RNFL thickness was the reason for the dense RPCs arrangement within the arcuate regions. However, our results revealed that the distribution rules of RCPs density do not follow RNFL rules, especially in temporal and nasal areas. The macula is a specialized region for high metabolic activity because of the greater density of cone photoreceptors, ganglion cell layer, and retinal pigment epithelial cell [24,25]. So, except for the structure-vascular relationship, the activity-vascular related correlation was another mechanism that can explain the distribution rules.

However, while we know the distribution rules of RPCs density, the parameter can be another useful index to identify optic neuropathies such as glaucoma. However, studies with larger samples are needed to determine in which region the earliest decrease of RPCs density happens.

There were several limitations in the study. The first is the scoring rules of large vessels. We graded the scores roughly according to the vascular size, but did not measure the exact vessel diameter. As the roles of arterioles and venules in supporting retinal tissue were different, the effect on the measurement might be also different, but we did not distinguish the arterioles or venules when grading large vessels in the current study. Another limitation is the relatively small sample size and wide age range. Further research with larger sample size and different age groups is needed to further assess the distribution and correlation of RPCs density and RNFL thickness in each area.

Conclusions

Our study assessed the distribution characteristics of RPCs density and RNFL thickness around the optic nerve. While we found the distribution rules of RPCs density, it might be another useful index to identify disease or follow disease progression using OCTA technology.

The relationship of distribution rules of RPCs density and RNFL thickness appeared to be not only vascular-structure related, but also activity-vascular related.

Declaration of Figures Authenticity

All figures submitted were created by the authors, who confirm that the images are original with no duplication and have not been previously published in whole or in part.

References:

1. Chan G, Balaratnasingam C, Xu J, et al. In vivo optical imaging of human retinal capillary networks using speckle variance optical coherence tomography with quantitative clinico-histological correlation. Microvasc Res. 2015;100:32-39

2. Mansoori T, Sivaswamy J, Gamalapati JS, Balakrishna N. Topography and correlation of radial peripapillary capillary density network with retinal nerve fibre layer thickness. Int Ophthalmol. 2018;38:967-74

3. Yu PK, Cringle SJ, Yu DY. Correlation between the radial peripapillary capillaries and the retinal nerve fibre layer in the normal human retina. Exp Eye Res. 2014;129:83-92

4. Mansoori T, Sivaswamy J, Gamalapati JS, et al. Measurement of radial peripapillary capillary density in the normal human retina using optical coherence tomography angiography. J Glaucoma. 2017;26:241-46

5. Jo YH, Sung KR, Yun SC. The relationship between peripapillary vascular density and visual field sensitivity in primary open-angle and angle-closure glaucoma. Invest Ophthalmol Vis Sci. 2018;59:5862-67

6. Yu PK, Balaratnasingam C, Xu J, et al. Label-free density measurements of radial peripapillary capillaries in the human retina. PLoS One. 2015;10:e0135151

7. Scoles D, Gray DC, Hunter JJ, et al. In-vivo imaging of retinal nerve fiber layer vasculature: Imaging histology comparison. BMC Ophthalmol. 2009;9:9

8. Rao HL, Yadav RK, Addepalli UK, et al. The ISNT rule in glaucoma: Revisiting with spectral domain optical coherence tomography. Acta Ophthalmol 2015; 93:e208-13

9. Pradhan ZS, Braganza A, Abraham LM. Does the ISNT rule apply to the retinal nerve fiber layer? J Glaucoma. 2016;25:e1-4

10. Mansoori T, Sivaswamy J, Gamalapati JS, Balakrishna N. Radial peripapillary capillary density measurement using optical coherence tomography angiography in early glaucoma. J Glaucoma. 2017;26:438-43

11. Mammo Z, Heisler M, Balaratnasingam C, et al. Quantitative optical coherence tomography angiography of radial peripapillary capillaries in glaucoma, glaucoma suspect, and normal eyes. Am J Ophthalmol. 2016;170:41-49

12. Scripsema NK, Garcia PM, Bavier RD, et al. Optical coherence tomography angiography analysis of perfused peripapillary capillaries in primary open-angle glaucoma and normal-tension glaucoma. Invest Ophthalmol Vis Sci. 2016;57:OCT611-20

13. Jia Y, Simonett JM, Wang J, et al. Wide-field OCT angiography investigation of the relationship between radial peripapillary capillary plexus density and nerve fiber layer thickness. Invest Ophthalmol Vis Sci. 2017;58:5188-94

14. Mase T, Ishibazawa A, Nagaoka T, et al. Radial peripapillary capillary network visualized using wide-field montage optical coherence tomography angiography. Invest Ophthalmol Vis Sci. 2016;57:OCT504-10

15. Chandrasekera E, An D, McAllister IL, et al. Three-dimensional microscopy demonstrates series and parallel organization of human peripapillary capillary plexuses. Invest Ophthalmol Vis Sci. 2018;59:4327-44

16. Alnawaiseh M, Lahme L, Müller V, et al. Correlation of flow density, as measured using optical coherence tomography angiography, with structural and functional parameters in glaucoma patients. Graefes Arch Clin Exp Ophthalmol. 2018;256:589-97

17. Cerdà-Ibáñez M, Duch-Samper A, Clemente-Tomás R, et al. Correlation between ischemic retinal accidents and radial peripapillary capillaries in the optic nerve using optical coherence tomographic angiography: Observations in 6 patients. Ophthalmol Eye Dis. 2017;9:1179172117702889

18. Ávila-Marrón E, Liscombe-Sepúlveda JP, Manfreda-Dominguez L, et al. Purtscher's retinopathy case report: Short posterior ciliary arteries contribution to radial peripapillary capillary system observed with optical coherence tomography angiography. Int Ophthalmol. 2019;39:2661-65

19. Poon LY, Solá-Del Valle D, Turalba AV, et al. The ISNT rule: How often does it apply to disc photographs and retinal nerve fiber layer measurements in the normal population? Am J Ophthalmol. 2017;184:19-27

20. Watanabe T, Raff MC. Retinal astrocytes are immigrants from the optic nerve. Nature. 1988;332:834-37

21. Fruttiger M. Development of the retinal vasculature. Angiogenesis. 2007;10:77-88

22. O'Sullivan ML, Puñal VM, Kerstein PC, et al. Astrocytes follow ganglion cell axons to establish an angiogenic template during retinal development. Glia. 2017;65:1697-716

23. Burne JF, Raff MC. Retinal ganglion cell axons drive the proliferation of astrocytes in the developing rodent optic nerve. Neuron. 1997;18:223-30

24. Provis JM, Penfold PL, Cornish EE, et al. Anatomy and development of the macula: Specialisation and the vulnerability to macular degeneration. Clin Exp Optom 2005;88:269-81

25. Bhavsar KV, Lin S, Rahimy E, et al. Acute macular neuroretinopathy: A comprehensive review of the literature. Surv Ophthalmol. 2016;61:538-65